# Visualization of the hygroscopic water distribution in an adsorbent bed by neutron radiography

Asano, Hitoshi
Takenaka, Nobuyuki
Fujii, Terushige
Nakajima, Takehiko

Journal logo

# Visualization and Void Fraction Distribution of Downward Gas-Liquid Two-Phase Flow in a Plate Heat Exchanger by Neutron Radiography

Hitoshi Asano*, Nobuyuki Takenaka, Toshiaki Wakabayashi, Terushige Fujii

*Department of Mechanical Engineering, Kobe University, 1-1 Rokkodai-cho, Nada-ku, Kobe 657-8501, Japan*

**Elsevier use only:** Received date here; revised date here; accepted date here

**Abstract**

Adiabatic vertically downward air-water two-phase flows in a commercial plate heat exchanger were visualized by a neutron radiography method as a non-destructive test in order to clarify the flow characteristics and the differences of the liquid distributions from those of the vertically upward flows. Flow behaviors in a single channel and a multi channel plate heat exchanger were investigated. From the visualized results of the flows in a single channel, it was shown that water fell down without a spreading at a lower gas volumetric flux of less than about 2 m/s. In the case of a higher gas volumetric flux above 2 m/s, liquid spread around the enlarged section and the liquid distribution in the main part of the heat exchanger seemed to be homogenous. Measured average void fractions for the air-water downward flows showed almost the same tendency as those for the upward flows in spite of the difference of the flow patterns. On the other hand, liquid distributions into 18 parallel channels were evaluated from the measured results of the liquid volumetric fractions in each channel. It was shown that the liquid distribution depended on the inlet liquid flow rate. However, the effect of the gas flow rate was a little. In the case of higher liquid flow rate, the liquid fraction became higher with a deeper channel due to a larger liquid momentum. However, in the case of a lower liquid flow rate, the opposite tendency was observed, i.e. the liquid fraction in the nearest channel to the inlet was higher.


*PACS: 87.59.B*
*Keywords* : Plate heat exchanger ; Gas-liquid two-phase flow ; Flow visualization ; Liquid distribution ; Neutron radiography

* Corresponding author. Tel.: +81-78-803-6122 ; fax: +81-78-803-6122 ; e-mail: asano@mech.kobe-u.ac.jp

## 1. Introduction

A plate heat exchanger is widely used in industrial processes, such as a chemical process, oil cooling system, and so on. In most cases, it is used for liquid single-phase flows. Recently, applications of plate heat exchangers to gas-liquid two-phase flows, such as an evaporator and condenser, have become of interest for a compactness and heat transfer performance improvement. A plate heat exchanger is made by brazing 20 to 280 sheets of stainless steel wavy plates. Working fluids flow through the gaps between these plates. The channel of each fluid is arrayed alternately, that is, a plate heat exchanger has many parallel channels. In the case where working fluids flow as gas-liquid two-phase mixtures, the dynamic flow behaviors greatly affect the heat transfer performance. In order to design or improve such heat exchanger, it is important to understand the liquid distribution not only in each channel but also into parallel channels. In particular, in the case where the inlet flow is a two-phase flow, the effects of the inlet flow conditions and inlet configuration on the liquid distribution might be large.

There are many papers on flow and heat transfer characteristics of liquid single-phase flows in plate heat exchangers and performance prediction methods with the consideration of geometric parameters were proposed by O. Charee, et al.[1]. However, there are a few papers on gas-liquid two-phase flow characteristics only in a single channel [2-4], and there is no paper on a plate heat exchanger with parallel channels, and a commercial one.

In such a case flow visualization is very efficient to know and clarify the conditions of the two-phase flow behaviors. The authors carried out visualization experiments of adiabatic gas-liquid and boiling two-phase flows in a single channel plate heat exchanger by thermal neutron radiography (H. Asano, et al. [5,6]). They showed in the visualized results of boiling two-phase flows that the liquid distributions were strongly affected by the inlet flow condition, i.e., either the liquid single-phase flow or the gas-liquid two-phase flow. Moreover, they conducted visualization experiments of upward air-water two-phase flows in a commercial one (H. Asano, et al. [7]).

In this study, to understand the existing conditions and problem in a gas-liquid two-phase flow application of a plate heat exchanger, adiabatic downward air-water two-phase flows in a commercial plate heat exchanger were visualized by thermal neutron radiography as a non-destructive test on flow structures. In the single channel experiments, the dynamic flow behaviors were visualized and the void fractions were calculated. On the other hand, in the multi channel experiments, the cross-sectional average liquid fractions in each channel were measured and the effect of the inlet conditions was considered.

## 2. Experimental apparatus

Flow visualization experiments were conducted by utilizing the JRR-3m thermal neutron radiography facility at JAERI (Japan Atomic Energy Research Institute) [8]. Two kinds of camera system were used according to the purpose of the visualization. A silicon intensified target (SIT) tube camera (30 fps, 512×512 pixels, 256(8 bit) intensity levels) was used for the dynamic behavior observations. On the other hand, a cooled charged-coupled-devise (C-CCD) still camera (1000×1018 pixels, 16384(14 bit) intensity levels) was used for the high-resolution measurements.

A schematic diagram of the experimental apparatus is shown in Fig.1. Water and air were used as the working fluids. Air was fed to a mixing section ***7*** from an air compressor through a pressure regulating valve ***4*** , a sonic nozzle ***5***, and a gas flow meter. Water in a tank ***1***, was fed by a pump ***2*** to the mixing section ***7*** through a cooler ***3*** to maintain the temperature, and a water flow meter. Two-phase flows which formed in the mixing section flew into the upper part of a test section placed vertically in the irradiation room. A commercial plate heat exchanger (Hisaka Works, Ltd., type BX) made from stainless wavy plates was used as the test section. The plate configuration is shown in Fig.2 (a). Wavy shape of 6.4 mm in pitch and 1.4 mm in height is formed by the pressing process of 0.45 mm thick sheets. The wave is inclined 30 degree to the horizontal line. A net-like channel is formed by a superposition of two plates with a bilateral symmetrical wavy shape. It can be seen in Figs. 3 (a) and (b) that water in the net-like channel is clearly visualized by neutron radiography. The average hydraulic diameter of the net-like

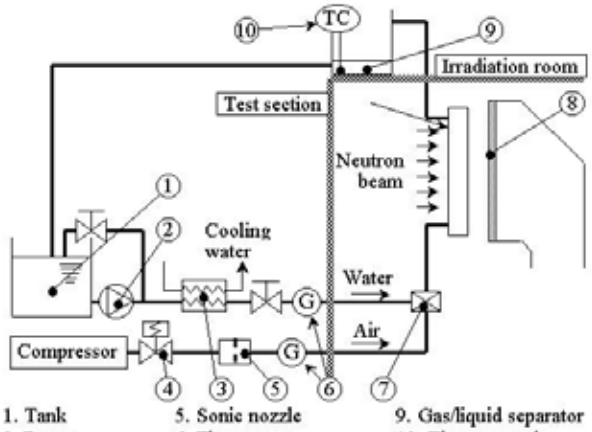


Fig.1 Schematic diagram of the experimental apparatus.

channel was 3.36 mm. Two-phase mixtures perpendicularly flew into the test section from the upper hole of a 23 mm diameter. A neutron beam was irradiated at the front face perpendicularly.

A vertical cross-section of the distributing header of a multi-channel test section is shown in Fig.2 (b). The multi-channel test section has 18 parallel channels. The hole in each plate forms the cylindrical distributing header of a 23 mm diameter and 69.7 mm length. A neutron beam was irradiated from the side of the test section in order to visualize each channel individually.

## 3. Image processing

Assuming that the brightness of a visualized image is proportional to the beam intensity on a scintillation converter and neglecting the attenuation term due to a gas phase, the brightness of two-phase flow image $S_{TP}(x,y)$, the image without a liquid $S_1(x,y)$, i.e., $\alpha(x,y)=1$, and the image full of a liquid $S_0(x,y)$, i.e., $\alpha(x,y)=0$, is expressed as the following equations [9].

$$S_{TP}(x,y)=G(x,y)\exp\left[-\rho_w\mu_{mw}t_w(x,y) - \{1-\alpha(x,y)\}\rho_L\mu_{mL}t_c(x,y)\right]+O_{TP}(x,y) \quad (1)$$

$$S_1(x,y)=G(x,y)\exp\left[-\rho_w\mu_{mw}t_w(x,y)\right]+O_1(x,y) \quad (2)$$

$$S_0(x,y)=G(x,y)\exp\left[-\rho_w\mu_{mw}t_w(x,y) - \rho_L\mu_{mL}t_c(x,y)\right]+O_0(x,y) \quad (3)$$

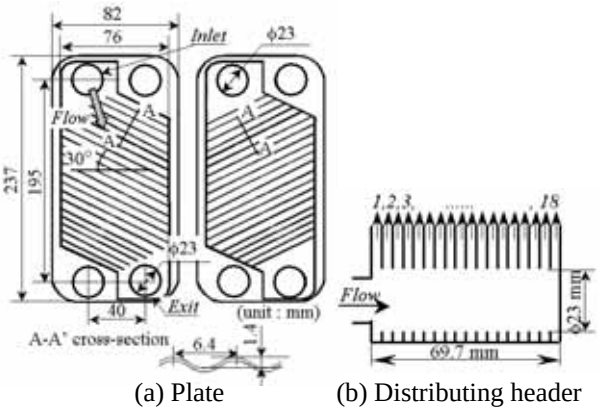


(a) Plate (b) Distributing header

Fig.2 Configuration of plate heat exchanger.

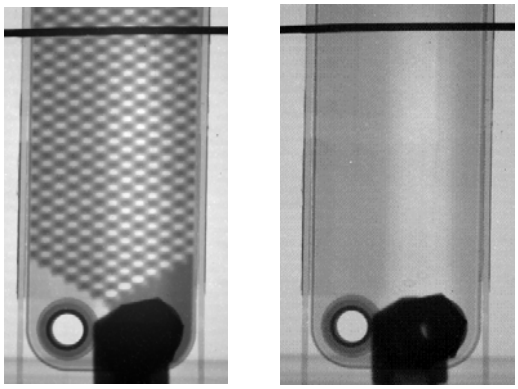

(a) Filled with liquid (b) Empty

Fig.3 Original image by neutron radiography.

where $\rho$ and $\mu_m$ are the density and mass attenuation coefficient, respectively, and those are physical properties of the objects. The function of $t$ is thickness along a neutron beam. The subscripts of $w$, $L$, and $c$ mean the wall, liquid, and conduit, respectively. $\alpha(x, y)$ mean the average void fraction along the neutron beam at coordinate (x, y). $G(x, y)$ is the gain and depends on the position due to a non-flatness of the initial beam intensity and of the sensitivity in a imaging system. $O_{TP}(x, y)$, $O_1(x, y)$ and $O_0(x, y)$ are the offset value in brightness. The offset value is caused by neutron scatterings in an object, optical scatterings in a neutron camera, and the dark current of an imaging system, that is, it depends on the flow conditions. Therefore, the offset value under each condition is necessary for quantitative measurements of the void fraction. Using equations (1) to (3), a two-dimensional void fraction distribution can be expressed as

$$\alpha(x,y)=\frac{ln\left[\frac{S_{TP}(x,y)-O_{TP}(x,y)}{S_0(x,y)-O_0(x,y)}\right]}{ln\left[\frac{S_1(x,y)-O_1(x,y)}{S_0(x,y)-O_0(x,y)}\right]} \quad (4)$$

The umbra method [9, 10] was applied to measure the offset values. A cadmium tape was used as a neutron absorber, and was placed at the front of the test section. Average brightness in the umbra of the cadmium tape was used as the offset value and it was measured under each condition.

## 4. Experimental results and discussion

### *4.1. Single channel*

Original visualized images by the SIT-tube camera are shown in Figs.4 (a) and (b). Each figure of (a) and (b) consists of four continuous frames at intervals of 1/30 seconds, respectively. Figure (a) shows the flow behavior of an upward flow with a liquid volumetric flux, $j_L$, of 0.05 m/s and a gas volumetric flux, $j_G$, of 1.1 m/s. Figure (b) is of a downward flow with a $j_L$ of 0.08 m/s and $j_L$ of 0.8 m/s. Brightness of the radiograph becomes lower with an increase of the attenuation of the neutron ray in an object. Darker part means a thicker liquid thickness. For the upward flow (Fig.4 (a)), the entrance was frequently filled with water (Fig.(i)), and air flew intermittently. When the entrance was filled with water, falling water was observed in the two-phase flow region. This flow pattern is classified as an intermittent flow. With an increase of the air flow rate, air began to flow continuously, and a reverse flow was not observed. On the other hand, for the downward flow (Fig.4 (b)), dispersion of the water in the enlarged section was weak. Most of the water seemed to flow in the left-side of the shortest pass between the inlet and exit. Such a flow might be based on the principle of the least energy dissipation by the friction and gravity. Water flow along both sides was also observed. This flow pattern is classified as a separated flow. It could be seen that there was a large difference of the flow pattern between the vertically upward and downward flow. However, at a higher air velocity, air was flowing continuously in both cases, and water seemed to be well dispersed. No remarkable difference in the flow pattern between the upward and downward flow was observed.

Two-dimensional void fraction distributions are shown in Figs.5 (a) to (f) in a grayscale. These results were calculated from the visualized images by the C-CCD camera with an exposure time of 2 seconds. White spot noises due to a direct irradiation on the CCD tips were removed by a morphological filter [11]. Non-homogenous liquid distributions were clearly seen under the condition with a lower air velocity. Liquid fraction was high around the shortest pass, especially, it was low at the left side at the $j_G$ less than 2 m/s. For the $j_G$ above 7 m/s the liquid distributions seemed to be homogenous.

Flow direction distributions of the cross-sectional average void fraction, $\overline{\alpha}$, are plotted in Fig.6 against the distance *y* indicated in Fig. 5(a). The void fraction periodically fluctuated in a constant range under every condition as shown in the previous results for the upward flows [7]. These fluctuations might be caused by the change in the cross-sectional area and liquid stagnation at the nodal points of the channel. Void fraction was almost stable in the net-like channel.

Average void fractions in the channel are calculated and plotted in Fig. 7. The horizontal and the vertical axis show a total volumetric flux, $j_L+j_G$, and a gas mean velocity, $j_G/\alpha$, respectively. Correlation curves for the upward flows are plotted by bold lines according to the flow patterns. An alternate long and short dash line shows the same on the homogenous flow model. These results for the downward flows agreed with those of the upward flows qualitatively and quantitatively.

### *4.2. Multi- channel*

Liquid distribution into parallel channels was evaluated from the liquid volumetric fraction in each channel. From a projection image in the direction parallel to the plates, the sum total of the liquid thickness in each channel can be measured individually from the two-phase flow image and the image without a liquid. Assuming that the volume of the conduit at an arbitrary cross-section is the same, the liquid volumetric fraction is equivalent to the

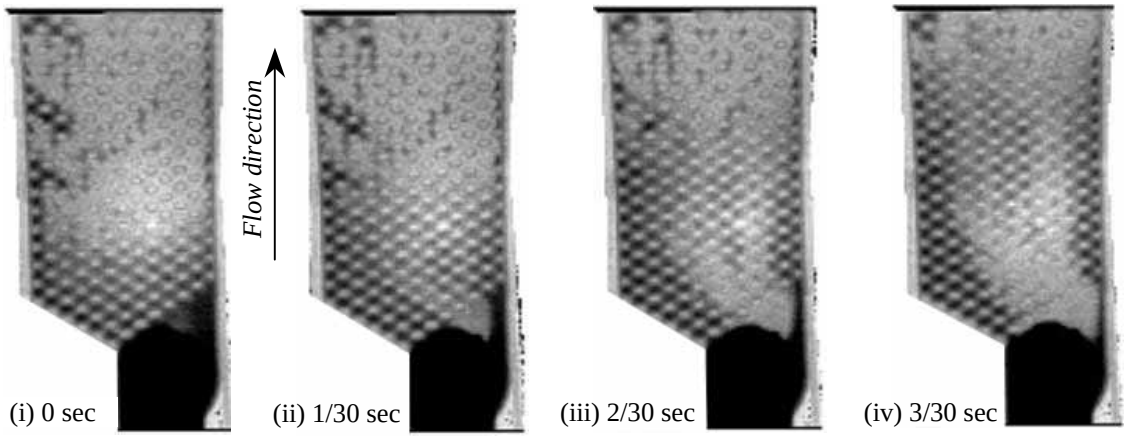


(a) Upward flow ($j_L$ = 0.05 m/s, $j_G$ = 1.1 m/s).

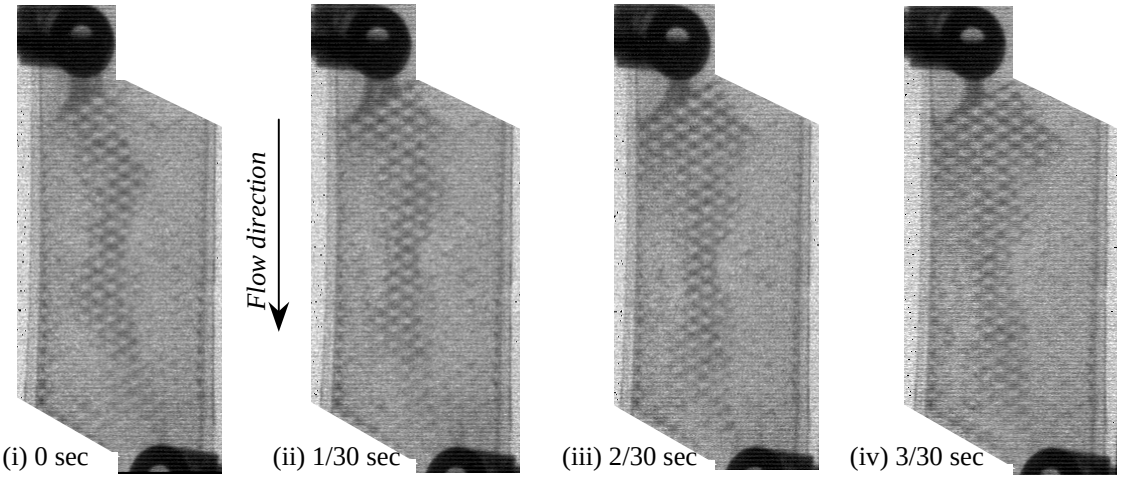


(b) Downward flow ($j_L$ = 0.08 m/s, $j_G$ = 0.8 m/s).

Fig.4 Original continuous image with 30 fps by SIT-tube camera.

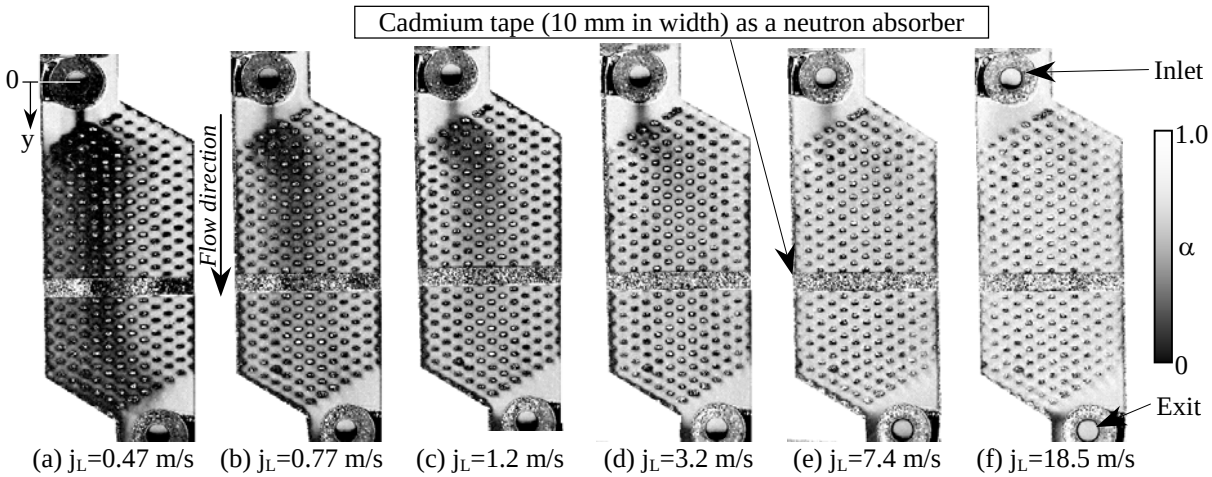


Fig.5 2D void fraction distribution calculated from still images by the cooled CCD camera ($j_L$ = 0.08 m/s).

ratio of the sum total of the liquid thickness in each channel.

Calculated results are plotted in Figs.8 (a) and (b). Vertical axis shows the liquid volumetric fraction normalized by the average value. In the Fig.8 (a), the liquid fraction was high at the both ends, and was a little lower with a deeper channel. However, at the higher $j_L$, the liquid distribution has the opposite tendency with the case of a lower $j_L$. Liquid fraction became higher with a deeper channel. This fact might be caused by the inertia force of the water in the header. For the upward two-phase flow, the effect of $j_G$ was large, because the flow pattern in the header was stratified and the liquid velocity increased with the increase of $j_G$. However, for the downward flow, since the water flows into each channel from the lower part of the header, the effect of $j_G$ on the liquid velocity in the header was little.

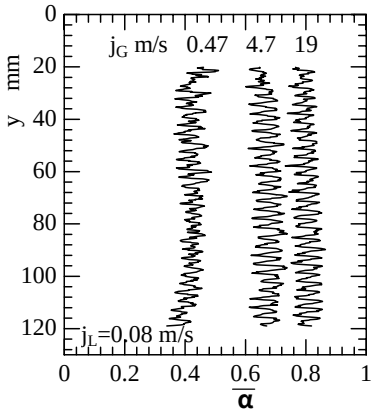


Fig.6 Flow direction distribution of cross-sectional void fraction.

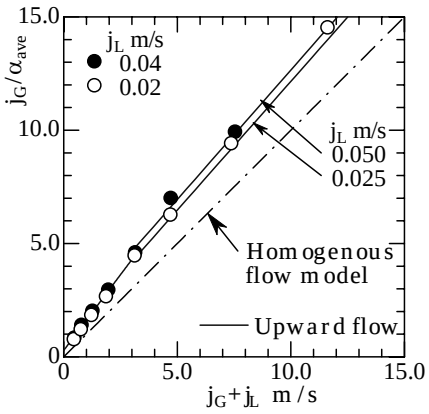


Fig.7 Average void fraction over the net-like channel.

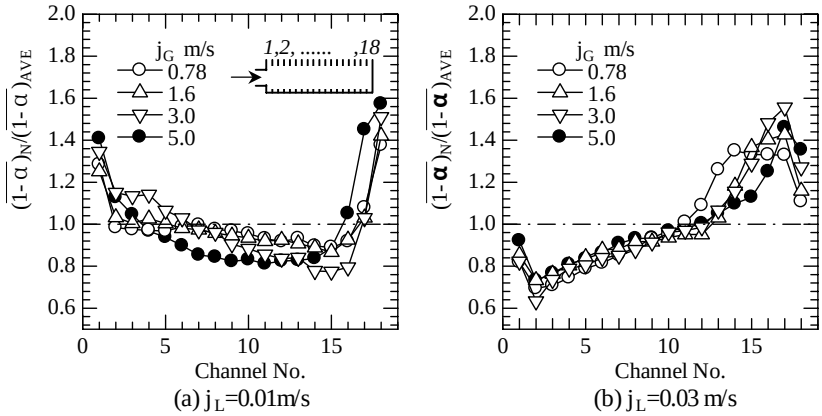


Fig.8 Liquid distribution in a multi channel plate heat exchanger.

## 5. Conclusions

As a non-destructive test of the flows in a plate heat exchanger, the adiabatic downward air-water two-phase flows in a commercial one were clearly visualized by the thermal neutron radiography. As a result, it was shown that the difference in the flow pattern between the upward and downward flows was observed at a low gas velocity condition, however the effect of the flow direction on the overall average void fraction in a single channel was little. Multi-channel experiments showed that the liquid distribution into the multi-channel strongly depended on $j_L$.

## References

[1] O. Charee, et al., Compact Heat Exchangers, Edizioni ETS, Pisa (2002) 207-212.

[2] Y. Shiomi, et al., Experimental Thermal and Fluid Science, 28 (2004) 231-235.

[3] C. Tribe, H. Müller-Steinhagen, Heat Transfer Engineering, 22-1 (2001) 5-11.

[4] C. Tribe, H. Müller-Steinhagen, ibid., 22-1 (2001) 12-21.

[5] H. Asano, et al., Experimental Thermal and Fluid Science, 28 (2004) 223-230.

[6] H Asano, et al., Proc. of the German-Japanese Workshop on Multi-Phase Flow (2002) B17-B28.

[7] H. Asano, et al., Proc. 5th Int. Conf. on Multiphase Flow on CD-Rom (2004) Paper No.172.

[8] M. Matsubayashi and A. Tsuruno, Neutron Radiography 4, Gordon and Breach Science Publishers (1992) 415-422.

[9] N. Takenaka, et al., Nondestructive Testing and Evaluation, 16 (2001) 345-354.

[10] H. Kobayashi, et al., J. of Nuclear Science and Technology, 29-11 (1992) 1-9.

[11] Y. Motomura, et al., Proc. of 5th World Conf. on Neutron Radiography (1997) 229-236.